

Electronic Supplementary Information (ESI)

**Integrated insights into Na<sup>+</sup> storage mechanism and electrochemical kinetics of ultrafine V<sub>2</sub>O<sub>3</sub>/S and N co-doped rGO composites as anodes for sodium ion batteries**

Leping Yang,<sup>†a</sup> Zihe Zhang,<sup>†a</sup> Lishuang Xia,<sup>a</sup> Yifei Zhao,<sup>a</sup> Feng Li,<sup>a</sup> Xu Zhang,<sup>a</sup> Jinping Wei,<sup>a</sup> Zhen Zhou<sup>\*ab</sup>

<sup>a</sup> School of Materials Science and Engineering, Institute of New Energy Material Chemistry, Renewable Energy Conversion and Storage Center (ReCast), Key Laboratory of Advanced Energy Materials Chemistry (Ministry of Education), Nankai University, Tianjin 300350, China. E-mail: [zhouzhen@nankai.edu.cn](mailto:zhouzhen@nankai.edu.cn)

<sup>b</sup> School of Chemical Engineering and Energy, Zhengzhou University, Zhengzhou 450001, China.

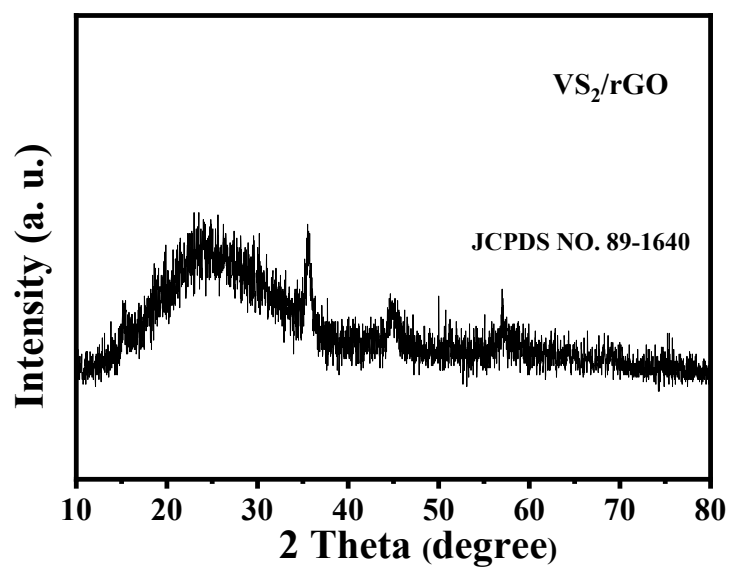


**Fig. S1.** XRD patterns of VS<sub>2</sub>/rGO.

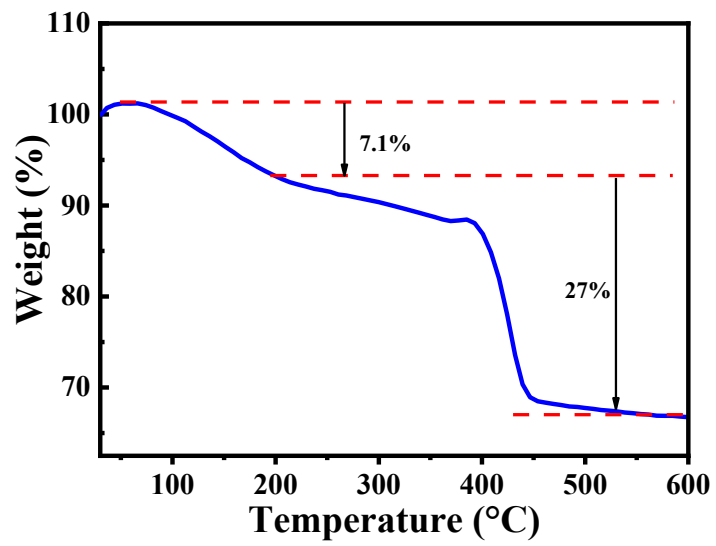


**Fig. S2.** TG-DTA curve of V<sub>2</sub>O<sub>3</sub>/S,N co-doped rGO composite in air with a heating rate of 5 °Cmin<sup>-1</sup> (30-600°C).

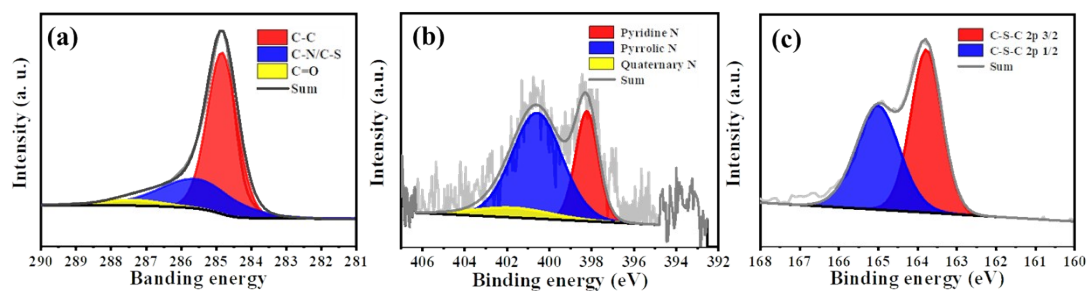


**Fig. S3.** High-resolution XPS of (a) C1s, (b) N1s and (c) S2p for rGO.

For high-resolution N1s spectra, three peaks are located at 398.2 eV (pyridine N), 400.5 eV (pyrrole N) and 401.4 eV (graphitic N), respectively.

For high-resolution C1s spectra, the highest peak is located at 284.8 eV represents  $sp^2$ -hybridized carbon (C-C). The other two peaks are situated at 285.35 eV (C-N/C-S) and 287.15 eV (C=O), respectively.

For high-resolution S2p spectra, two peaks are located at 163.7 eV and 165 eV, which are assigned to  $-C-S-C-$  heterocyclic configuration.

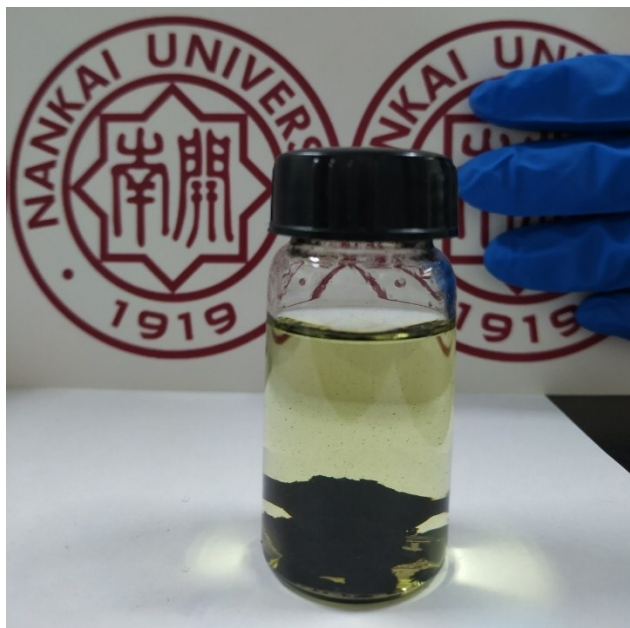


**Fig. S4.** The generated VS<sub>2</sub>/rGO gels after hydrothermal reaction.

The fluid is transparent with the color of faint yellow, and the VS<sub>2</sub>/rGO composite forms a black gel-like block at the bottom of bottle.

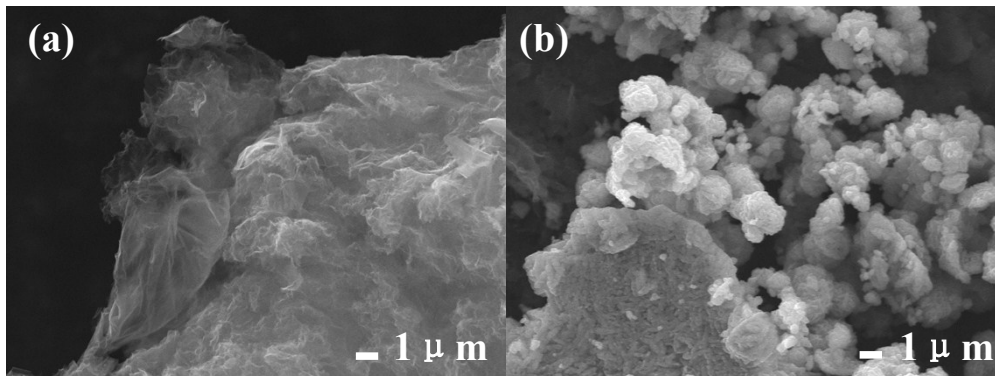


**Fig. S5.** SEM images of (a) rGO and (b) V<sub>2</sub>O<sub>3</sub>.

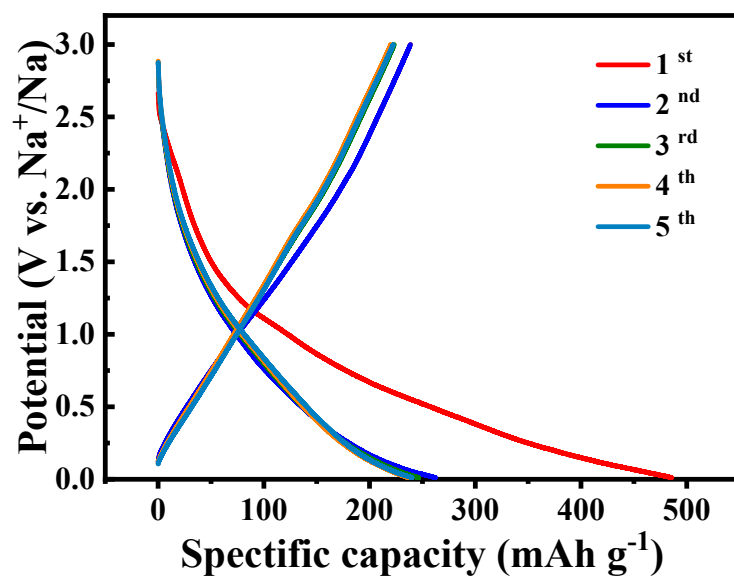


Fig. S6. Discharge and charge curves of V<sub>2</sub>O<sub>3</sub>/S,N co-doped rGO.

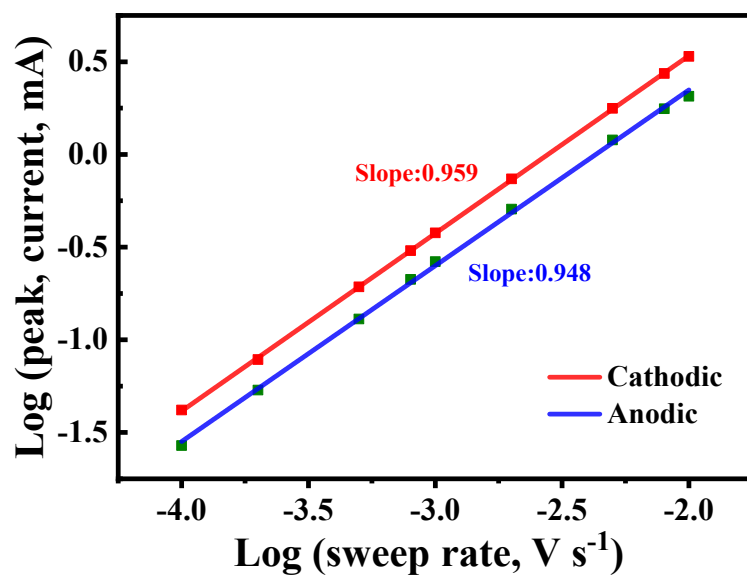
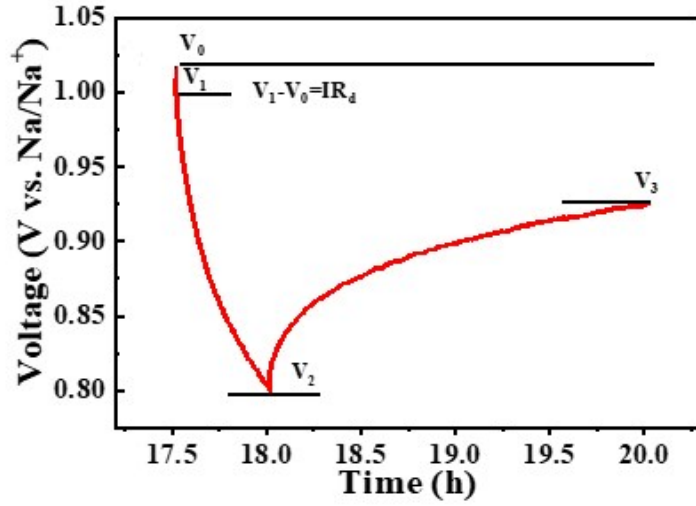


Fig. S7. The linear relationship between the log  $i$  and log  $v$ .





**Fig. S8.** (a) An enlarged discharge pulse of the GITT for  $V_2O_3/S,N$  co-doped rGO.

### $D_{Na^+}$ diffusion coefficient calculation<sup>1,2</sup>

According to the equation:

$$D_{Na^+} = \frac{4}{\pi} \left( \frac{m_B V_m}{M_B S} \right)^2 \left( \frac{\Delta V_s}{\tau \left( \frac{dV}{d\sqrt{\tau}} \right)} \right)^2, \quad \left( \tau \leq \frac{l}{D_{Na^+}} \right)$$

If  $V$  vs.  $\sqrt{\tau}$  shows straight-line behavior during the duration of the current pulse, then this equation can be transformed into:

$$D_{Na^+} = \frac{4}{\pi \tau} \left( \frac{m_B V_m}{M_B S} \right)^2 \left( \frac{\Delta V_s}{\Delta V_\tau} \right)^2, \quad \left( \tau \leq \frac{l}{D_{Na^+}} \right)$$

$\tau$ : current pulse time (sec).

$m_B$ : mass of B in sample (g).

$V_m$ : molar volume of B ( $\text{cm}^3/\text{mol}$ ).

$S$ : contact surface area ( $\text{cm}^2$ ).

$l$ : the thickness of electrode.

$V_0$ : the original cell voltage.

$V_1$ : the cell voltage after IR drops.

$V_2$ : the cell voltage after removing the current.

$V_3$ : the final cell voltage.

$\Delta V^t$ : the difference of the cell voltage,  $\Delta V^t = V_1 - V_2$ .

$\Delta V_s$ : the difference in the open circuit voltage measured at the end of the relaxation period for two successive steps (V),  $\Delta V_s = V_0 - V_3$ .

$I$ : current density (A).

$R_d$ : total resistance

## References

- 1 Y.-E. Zhu, L. Yang, X. Zhou, F. Li, J. Wei and Z. Zhou, *J. Mater. Chem. A*, 2017, 5, 9528-9532.
- 2 Z. Shen, L. Cao, C. D. Rahn and C. Wang, *J. Electrochem. Soc.*, 2013, 10, 1842-1846.

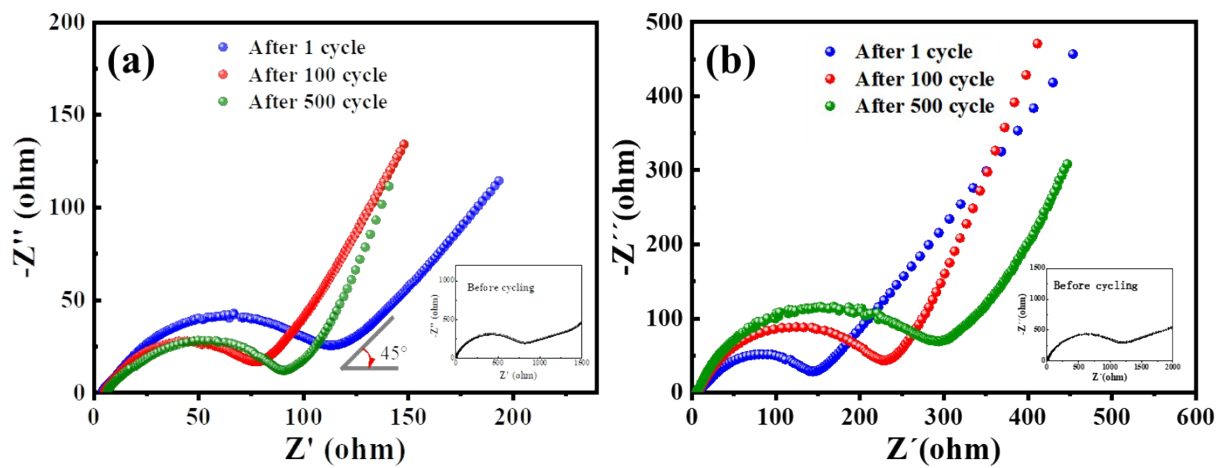


**Fig. S9.** EIS of (a)  $V_2O_3/S,N$  co-doped rGO and (b)  $V_2O_3$  before cycling and after 1 cycle, 100 cycles and 500 cycles.

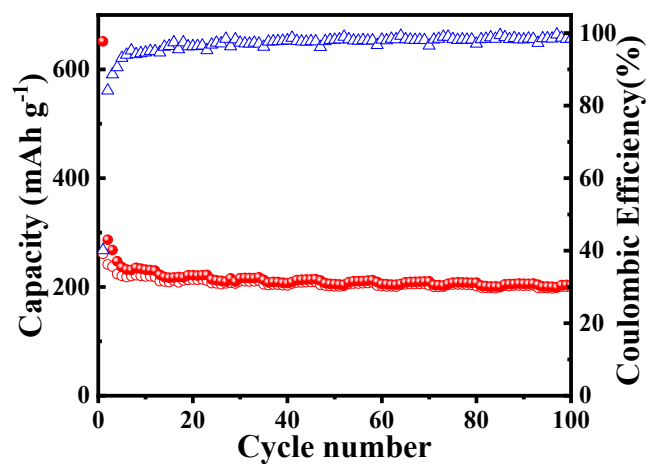


**Fig. S10.** Cycle performance of V<sub>2</sub>O<sub>3</sub>/S,N co-doped rGO at 0.2 A g<sup>-1</sup>.

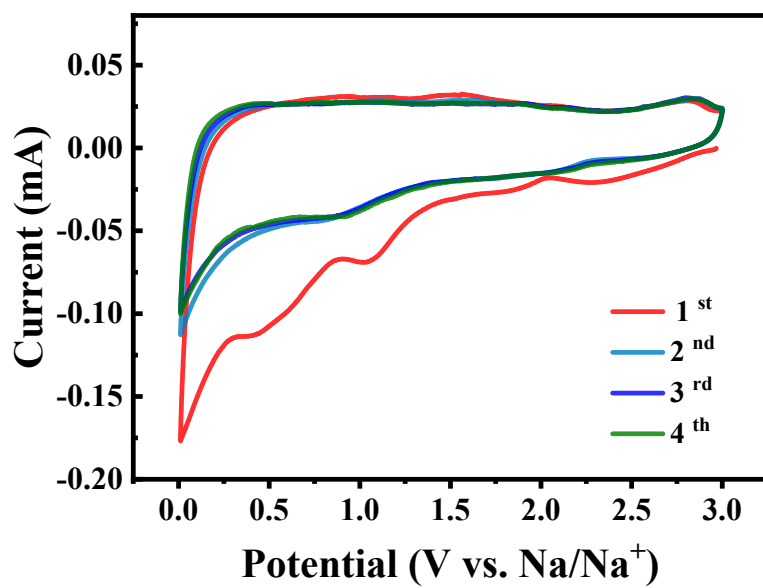


**Fig. S11.** CV curves of V<sub>2</sub>O<sub>3</sub>/S,N co-doped rGO for the initial four cycles.

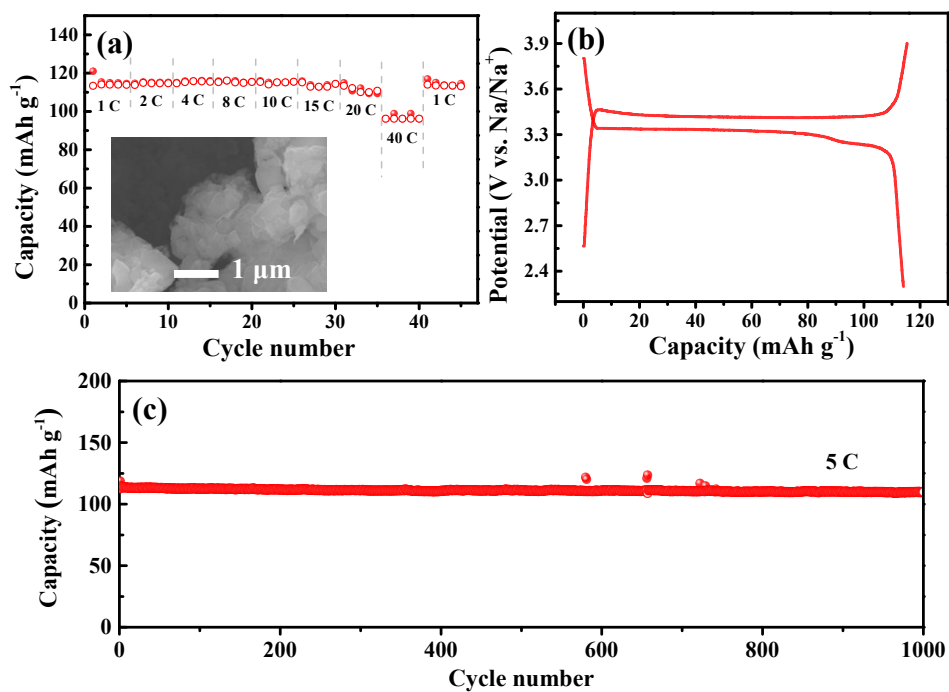


**Fig. S12.** (a) Rate performance of  $\text{Na}_3\text{V}_2(\text{PO}_4)_3@\text{rGO}$ , and the inset pattern is the SEM of  $\text{Na}_3\text{V}_2(\text{PO}_4)_3@\text{rGO}$ . (b) The charge-discharge curves of  $\text{Na}_3\text{V}_2(\text{PO}_4)_3@\text{rGO}$ . (c) The cycle stability of  $\text{Na}_3\text{V}_2(\text{PO}_4)_3@\text{rGO}$  (1 C= $128\text{ mAh g}^{-1}$ ).

**Table S1.** The lattice constants of bulk  $V_2O_3$  and  $NaV_2O_3$  unit cell calculated by DFT. Length a,b and c is in Å, angle  $\alpha$ ,  $\beta$  and  $\gamma$  is in degree, and the volume is in Å<sup>3</sup>.

	space group	a	b	c	$\alpha$	$\beta$	$\gamma$	volume
$V_2O_3$	R-3c	4.81	4.81	14.51	90.0	90.0	120.0	291.2
$NaV_2O_3$	R-3c	4.92	4.92	16.10	90.0	90.0	120.0	336.9

